

Correction of Radial Load Distribution Integral for Radial Bearings

Yu Hou

Beijing Jiaotong University <https://orcid.org/0000-0003-0565-5367>

Yi Yin

Beijing Jiaotong University

Xi Wang (✉ wangxi@bjtu.edu.cn)

<https://orcid.org/0000-0001-8329-5489>

Original Article

Keywords: Radial load distribution, Corrected radial load distribution integral, Radial bearing, Small load zone

Posted Date: June 22nd, 2020

DOI: <https://doi.org/10.21203/rs.3.rs-36826/v1>

License:   This work is licensed under a Creative Commons Attribution 4.0 International License.

[Read Full License](#)

Title page

Correction of Radial Load Distribution Integral for Radial Bearings

Yu Hou, born in 1994, is currently a PhD candidate at *School of Mechanical, Electronic and Control Engineering, Beijing Jiaotong University, China*. His research interests include structural health monitoring and mechanical properties of rolling bearings.
E-mail: 17116391bjtu.edu.cn

Yi Yin, born in 1990, is currently a postdoctoral fellow at *School of Mechanical, Electronic and Control Engineering, Beijing Jiaotong University, China*.

Xi Wang, born in 1976, is currently a professor and a PhD candidate supervisor at *School of Mechanical, Electronic and Control Engineering, Beijing Jiaotong University, China*. His main research interests include structure reliability and optimization of high-speed train.
Tel.: +86 10 51683195; E-mail: wangxi@bjtu.edu.cn

Corresponding author: Xi Wang E-mail: wangxi@bjtu.edu.cn

ORIGINAL ARTICLE

Correction of Radial Load Distribution Integral for Radial Bearings

Yu Hou¹ • Yi Yin¹ • Xi wang¹

Received June xx, 202x; revised February xx, 202x; accepted March xx, 202x

© Chinese Mechanical Engineering Society and Springer-Verlag Berlin Heidelberg 2017

Abstract: The radial load distribution integral is corrected for radial bearings. The error of Harris integral method for calculating the radial load distribution is analysed. The error is found absolutely caused by the inaccurate values of the radial load distribution integral given by Harris. Based on the extent of the load zone, the radial load distribution integral is corrected by three stages. The corrected radial load distribution integral is capable of calculating the load distribution of a bearing with a small load zone caused by a light external load or a great radial clearance. The corrected radial load distribution integral is found affected by the number of rolling elements. According to the variation of the number of rolling elements participating in the radial load transfer, the corrected radial load distribution integral can be divided into different phases. Some specific numerical examples are shown to illustrate the performance of the corrected radial load distribution integral. The comparison between the results obtained from the corrected radial load distribution integral and Harris integral shows the higher accuracy and superiority of the corrected radial load distribution integral.

Keywords: Radial load distribution • Corrected radial load distribution integral • Radial bearing • Small load zone

1 Introduction

When a radial ball or roller bearing is subjected to a radial load, the load is transferred from one raceway to another through the rolling elements. In this transfer process, the rolling elements are not equally loaded. This uneven load distribution is affected by the amplitude of the external load and the geometry of the rolling bearing [1] and plays a significant role on the operating characteristics of a bearing [2], such as the static carrying capacity [3,4], dynamic vibration [5–8], radial stiffness [5,9–12] and fatigue life [1,3,13–15].

✉ Xi Wang
wangxi@bjtu.edu.cn

To determine the radial load distribution, Stribeck [16] first derived an equation to calculate the maximum load on a rolling element of a ball bearing with zero radial clearance. A radial load distribution integral was proposed by Sjövall [17] to calculate the load distribution for nonzero clearances. The integral value is affected by the type of contact in a bearing and the ratio of the radial clearance to the ring radial shift so that the variables of the elliptic integral were introduced into the calculation. This integral is referred to as the Sjövall integral. Based on Sjövall's research, Harris [1] proposed a load distribution factor and adjusted the values of the radial load distribution integral by a numerical method which is called Harris integral in this paper. To obtain the integral value more easily, Oswald et al. [14] and Houper [18] used different polynomials to fit the relation of integral vs. the load distribution factor. A coefficient for the boundary external radial load was defined by Tomović [2,19] to ensure the number of the active rolling elements participating in the external load transfer. Without a calculation of the contact stiffness, Ren et al. [20] proposed a mathematical model in which only the deformations and geometric parameters of the bearing were used to determine the radial load distribution. Moreover, the bearing was considered a mass–spring–damper system, and the load distribution was calculated by multi-body nonlinear dynamic models by Petersen et al. [5,11] and Sawalhi et al. [21,22]. In addition, a comprehensive explicit dynamic finite element model [23] was used to analyse the dynamic contact forces in rotational bearings. Although all the methods are capable of calculating the radial load distribution, most of these methods have specific application conditions. For example, the load zone is assumed to be π and fixed in Stribeck's equation [16], which means Stribeck's method is not suitable for the calculation

¹ School of Mechanical, Electronic and Control Engineering, Beijing Jiaotong University, Beijing, 100044, China

of the bearings with a nonzero clearance. The discrete models proposed by Tomović [2,19] and Ren et al. [20] cannot be used to obtain the angle scope of the load zone while the dynamic models [11,21] are mostly used for vibration analysis and defect identification. Due to its simplicity, the method based on the load distribution integral has been widely used in many aspects of bearings [14][24][18][25].

However, several open questions remain for calculating the load distribution using the existing integral values. First, in the load distribution result obtained by the values of Sjövall integral or Harris integral, the sum of the vertical components of the calculated rolling element loads is not equal to the external radial load [1,19,20]. This calculation error cannot be neglected if the calculated load is used to predict some critical parameters such as fatigue life [25]. Second, when the load distribution factor is greater than 0 and less than 0.1, the value of the Harris integral or the way to calculate the integral are not given in previous studies. It indicates that the current integral method is not applicable for the small load zone situation caused by the light external load or great clearance[1]. The skidding of the rolling elements often occurs and results in smearing type of surface damage under light load situation [26], while the bearing tends to early failure operating with a great clearance [14].

In this paper, the correction for radial load distribution integral is proposed. The radial load distribution for point and line contacts are accurately obtained especially for the light load or great clearance conditions. Several numerical examples of commercial bearings are given to illustrate the impact of corrected load distribution integral.

2 Initial Assumptions

Figure 1 shows the geometries of the radial ball and roller bearings to calculate the radial load distribution. To achieve a practically applicable mathematical model and reduce ambiguous issues, some necessary assumptions should be presented:

1) Deformation only occurs at the individual contacts between the rolling elements and raceways. It complies with the Hertz elastic contact theory, other parts are absolutely rigid [1].

2) The bearing is subjected to a static load. The dynamic load distribution is considered the same as the static load distribution because, in most applications, the speeds of rotation are almost not as great as to cause ball or roller inertial force of sufficient magnitude to significantly affect the load distribution [13].

3) An external radial load F_r is downward applied to the inner ring of the bearing, and the outer ring is radially fixed.

4) For purposes of identifying and locating the position of the rolling elements, the bottom rolling element is set to 0, and the others are numbered clockwise as 1, 2, \dots , j , \dots , $Z-1$, where Z is the total number of rolling elements. The rolling element 0 is located in the line of the loading direction of F_r .

5) The unit azimuth angle β is constant for a bearing with fixed number of rolling elements, which is separated by a cage and calculated by the following formula:

$$\beta = \frac{2\pi}{Z} \quad (1)$$

According to the above assumptions, the load distribution is symmetrical with respect to the line of the loading direction, and the most loaded rolling element is the rolling element 0.

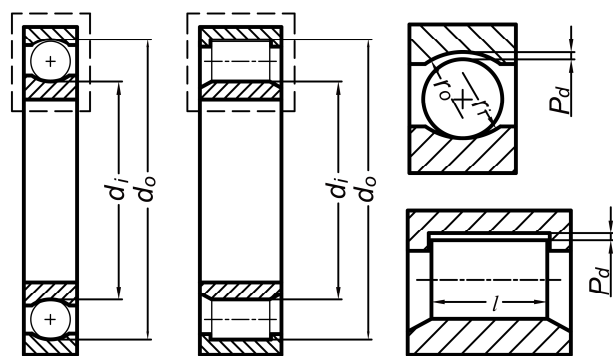
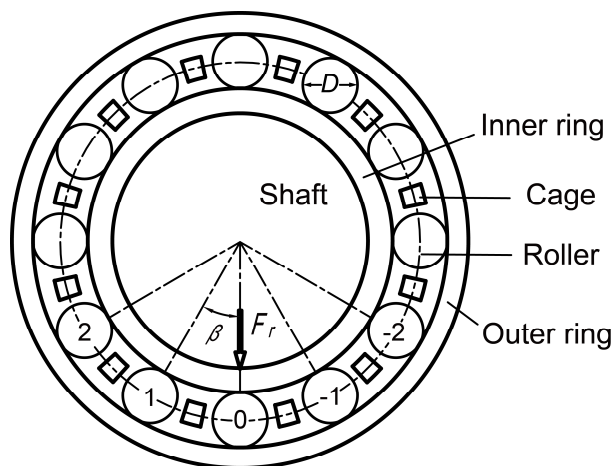


Figure 1 The structure and geometric parameters of the radial ball and roller bearing.

3 Harris Method to Calculate the Radial Load Distribution

3.1 Harris Radial Load Distribution Model and Integral

Based on the method proposed by Sjövall [17], Harris presented a comprehensive model and radial load distribution integral $J_r(\varepsilon)$ to calculate the radial load distribution using the load-deflection relationships [1].

For a bearing with rigid support under the radial loads, the radial deflection δ_j of the rolling element at the azimuth location $\varphi_j = j\beta$ is expressed by

$$\delta_j = \delta_r \cos \varphi_j - \frac{1}{2} P_d \quad (2)$$

where δ_r is the unknown inner ring radial shift occurring at $\varphi_0 = 0$ and P_d is the internal diametral clearance. In terms of maximum deformation δ_{\max} , δ_j can be rearranged as follows:

$$\delta_j = \delta_{\max} \left[1 - \frac{1}{2\varepsilon} (1 - \cos \varphi_j) \right] \quad (3)$$

where

$$\varepsilon = \frac{1}{2} \left(1 - \frac{P_d}{2\delta_r} \right) \quad (4)$$

ε is defined as the load distribution factor. From Eq. (4), the angular extent of the half load zone ψ_l is determined by the diametral clearance as follows:

$$\psi_l = \cos^{-1} \left(\frac{P_d}{2\delta_r} \right) \quad (5)$$

According to the load-deflection relationship of a rolling element-raceway contact expressed by

$$F_j = K \delta_j^n \quad (6)$$

and

$$\frac{F_j}{F_{\max}} = \left(\frac{\delta_j}{\delta_{\max}} \right)^n \quad (7)$$

where F_j is the radial load on the rolling element j and F_{\max} is the maximum distributing radial load and is equal to F_0 here. Number $n = 3/2$ for ball bearings, and $n = 10/9$ for roller bearings. K is a series of stiffnesses of the inner and outer raceway contact deformation. The calculation of K is illustrated in the Appendix.

From Eqs. (3), (6) and (7), the rolling element load F_j at any rolling element position can be given in terms of the maximum rolling element load F_{\max} by

$$F_j = F_{\max} \left[1 - \frac{1}{2\varepsilon} (1 - \cos \varphi_j) \right]^n \quad (8)$$

For static equilibrium, the external radial load must equal the sum of the vertical components of the rolling element loads:

$$F_r = \sum_{j=0}^{j=Z-1} F_j \cos \varphi_j \quad (9)$$

or

$$F_r = F_{\max} \sum_{j=0}^{j=Z-1} \left[1 - \frac{1}{2\varepsilon} (1 - \cos \varphi_j) \right]^n \cos \varphi_j \quad (10)$$

Introducing the radial load distribution integral $J_r(\varepsilon)$, Eq. (10) can be expressed by

$$F_r = Z F_{\max} J_r(\varepsilon) \quad (11)$$

where

$$J_r(\varepsilon) = \frac{1}{2\pi} \int_{-\psi_l}^{+\psi_l} \left[1 - \frac{1}{2\varepsilon} (1 - \cos \psi) \right]^n \cos \psi d\psi \quad (12)$$

In Harris' procedure, the radial integral $J_r(\varepsilon)$ has been given numerically for various values of the load distribution factor ε and shown in *Table 7.1* and *Figure*

7.2 in Ref. [1]. From Eqs. (2) and (6), F_{\max} can be expressed as follows:

$$F_{\max} = K\delta_0^n = K\left(\delta_r - \frac{1}{2}P_d\right)^n \quad (13)$$

Therefore, Eq. (13) is introduced into Eq. (11),

$$F_r = ZK\left(\delta_r - \frac{1}{2}P_d\right)^n J_r(\varepsilon) \quad (14)$$

For a given bearing with a given clearance under a given load, δ_r is the only unknown value. Harris et al. [1] presented that Eq. (14) may be solved by trial and error. A value of δ_r is first assumed, and ε is calculated from Eq. (4). Furthermore, the value of $J_r(\varepsilon)$ can be yielded from the curves of $J_r(\varepsilon)$ vs. ε provided by Harris as shown in Table 7.1 and Figure 7.2 in Ref. [1]. If Eq. (14) does not balance, then the process is repeated. When Eq. (14) balances, δ_r obtains its value. Then, F_j could be calculated by Eqs. (8) and (13).

3.2 Error of Harris Model and Integral

In Harris model mentioned above, three formulas, Eqs. (4) (12) and (14), significantly determine the radial load distribution in a radial bearing. During the calculation using these formulas, as input parameters, the external radial load F_r , total number of rolling elements Z , radial clearance P_d and contact stiffness K do not affect the accuracy of the calculation. However, some calculation errors exist and vary with these input parameters during the calculation of radial load distribution by Harris integral model [1,19,20]. The errors can only be caused by the inaccurate values of $J_r(\varepsilon)$ evaluated numerically by Harris. The calculation error is defined as the difference between the sum of the vertical components of distributed load F_j and the external radial load F_r , i.e.:

$$Error = \frac{\sum_{j=0}^{Z-1} F_j \cos \varphi_j - F_r}{F_r} \times 100\% \quad (15)$$

Some examples are given to figure out the influences of Harris integral to the calculation error of Harris method. The values of Harris integral in Table 7.1 and Figure 7.2 from

Ref. [1] are used in these examples. When the other input parameters are fixed ($F_r = 5000\text{N}$, $P_d = 0.04\text{mm}$, $K = 278630\text{N/mm}^n$, $n = 3/2$ for point contact and $n = 10/9$ for line contact), the errors of Harris method varying with the total number of rolling elements is shown in Figure 2. It is found that the errors of Harris method for both roller and ball bearings become smaller with the increase of the total number of the rolling elements overall, while the values and fluctuation of the error for roller bearing are greater than for ball bearing. The maximum error of these numerical examples is up to nearly 12% when the bearing is a roller bearing with 6 rollers. Moreover, according to the different number of loaded rolling elements, the errors can be divided into different phases. For example, 3 rollers participate in the radial load transfer and the error shows a negative-positive-negative trend when $Z=6-12$ for the roller bearing. In all of the phases, the variation trends of the errors vs. the rolling element number Z are absolutely the same.

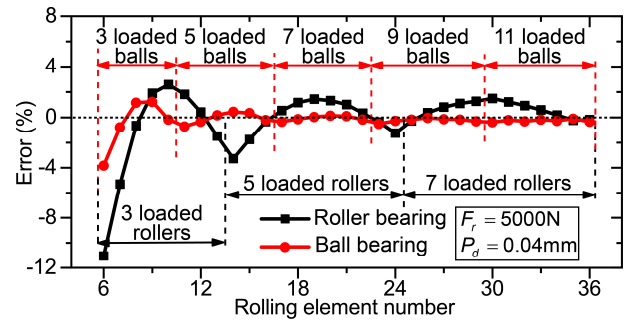


Figure 2 Errors of Harris method vs. the total number of rolling elements.

The errors of Harris method under different external radial loads and radial clearances are shown in Figure 3. A roller bearing with 10 rollers and $K = 278630\text{N/mm}^{10/9}$ is chosen in these examples. The error of Harris method is considered to raise with the growth of F_r by Ren et al. [20], however, some different trends are indicated in Figure 3. According to different load zone extents, the load distribution in a radial bearing with 10 rollers is divided into six phases as shown in Figure 4. Phase I to VI, respectively corresponding to only one rolling element participating in load transfer to all rolling elements participating in load transfer, introduce the evolution of the load distribution with the load distribution factor ε . These phases are marked in Figure 3. As shown in Figure 3(a), overall, a bigger radial clearance indicates a severer error when $P_d > 0$, and the error decreases with the increase of the external radial load. The maximum error with a value of about 17.5% appears when there are the maximum P_d and minimum F_r .

Differing from the case of positive clearance, the maximum values of Harris method error are no more than 1% and hardly affected by the values of the clearance when $P_d < 0$ as shown in Figure 3(b). For different radial clearances, although the scopes of the same load phase are different, the variation and values of the error varying with F_r are almost the same in the same load phase. For example, in Figure 3(a), the error shows a negative-positive-negative trend varying with F_r in all of the phase II, while the error tends to vary from negative values to zero in all of the phase III. In Figure 3(b), the errors in all phase VI are absolutely zero, and the error shows a positive-negative-positive trend in all of the phase IV, while the error decreases with the increase of F_r in all of the phase III. It is indicated that the error of Harris method is significantly affected by the load zone extent i.e. the load distribution factor ε .

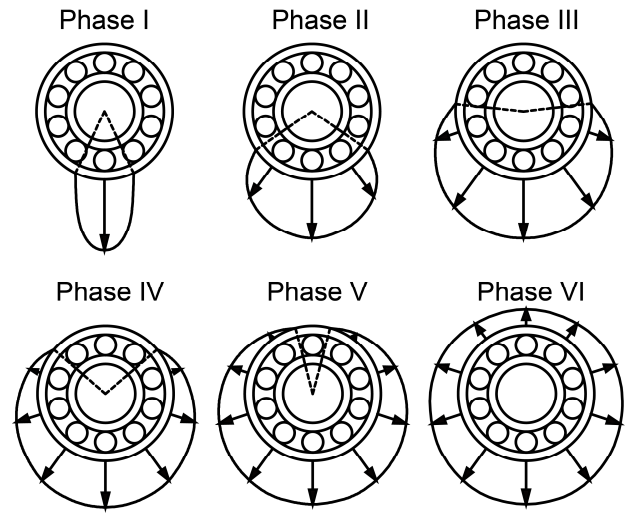


Figure 4 Six load phases of the radial bearing with 10 rolling elements.

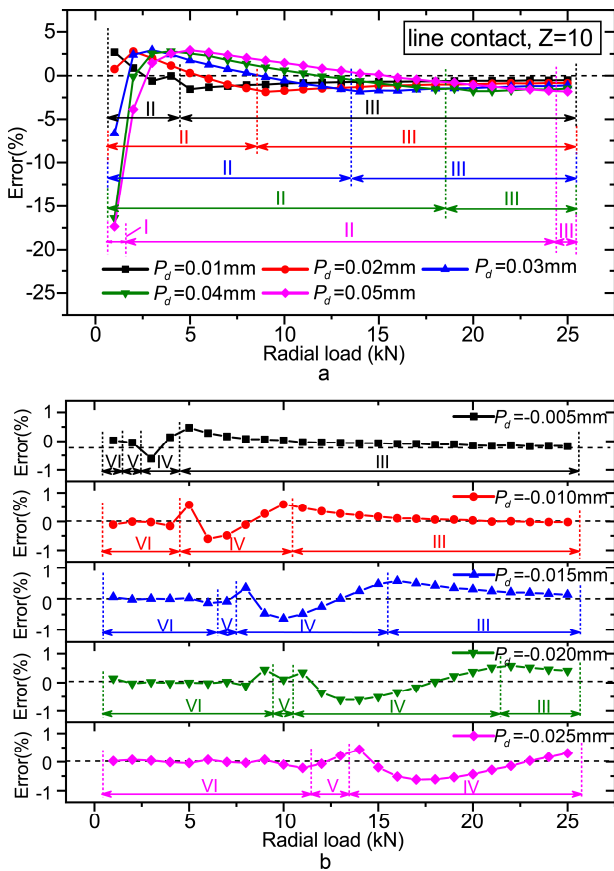


Figure 3 Errors of Harris method vs. the external radial loads and radial clearances, (a) positive clearances and (b) negative clearances.

With the load distribution factor ε as the independent variable and the error as the dependent variable, Figure 5 shows the error varying with ε for a roller bearing with 10 rollers. Different load phases are marked in Figure 5. It is shown that the error varies with ε following different trends in different load phases when $\varepsilon < 1$ and almost keeps a values of zero when $\varepsilon > 1$. Moreover, the smaller the load distribution factor ε is, the severer the variation scope and the maximum value of the errors are. Because the input parameters do not affect the accuracy of the calculation, all of the errors are absolutely caused by the inaccurate values of $J_r(\varepsilon)$ evaluated numerically by Harris. Besides, when $0 < \varepsilon < 0.1$, the values of $J_r(\varepsilon)$ is not given by Harris, which implies Harris integral method does not apply to the situation of a small load zone of $\psi_l < 36.87^\circ$ (calculated by Eq. (4) and (5) when $\varepsilon < 0.1$) caused by a light external load or a great radial clearance. So, it is necessary to correct $J_r(\varepsilon)$ for calculating the load distribution of radial bearings accurately by integral method.

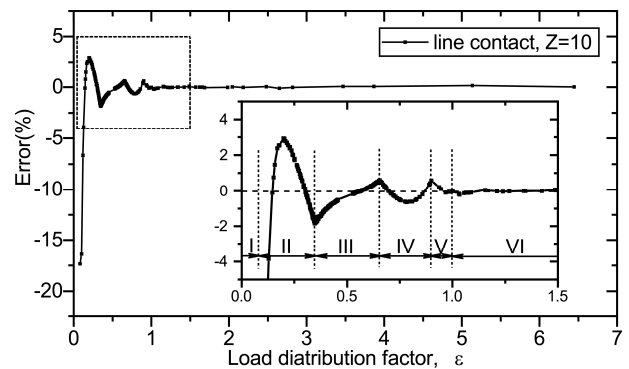


Figure 5 Error of Harris method vs. the load distribution factor

for a roller bearing with 10 rollers.

4 Correction of Radial Load Distribution Integral

4.1 Calculation of Load Distribution Integral by Discrete Method

A discrete method is used to correct the radial load distribution integral here. The equilibrium between the external radial load and the sum of the vertical components of the rolling element loads can be expressed in two forms: discrete form as Eq. (10) and integral form as Eq. (11). Comparing these two formulas, the radial load distribution integral can be expressed by discrete form:

$$J_r(\varepsilon) = \frac{1}{Z} \sum_{j=0}^{j=Z-1} \left[1 - \frac{1}{2\varepsilon} (1 - \cos \varphi_j) \right]^n \cos \varphi_j \quad (16)$$

However, because of the upper and lower limits of the summation in Eq. (16), this formula is only suitable for the case of $\varepsilon > 1$ i.e. the situation of all of the rolling elements participating in the load transfer. To calculate the values of $J_r(\varepsilon)$ when $\varepsilon < 1$, the number of active rolling elements need to be ensured, and the upper and lower limits of the summation in Eq. (16) need to be adjusted. When $\varepsilon < 1$, it is assumed that the rolling element at the two ends of the load zone are numbered k and $Z-k$. Thus, in the load zone, the number of rolling elements participating in the load transfer is $2k+1$ and $j=0, 1, Z-1, 2, Z-2, \dots, k, Z-k$. The integral $J_r(\varepsilon)$ for $\varepsilon < 1$ can be expressed as

$$J_r(\varepsilon) = \frac{1}{Z} \left\{ \sum_{j=0}^k \left[1 - \frac{1}{2\varepsilon} (1 - \cos \varphi_j) \right]^n \cos \varphi_j + \sum_{j=Z-k}^{Z-1} \left[1 - \frac{1}{2\varepsilon} (1 - \cos \varphi_j) \right]^n \cos \varphi_j \right\} \quad (17)$$

As long as the value of k is ensured, the value of $J_r(\varepsilon)$ can be calculated by Eq. (17). From Eq. (4) and Eq. (5), the relationship between the angular extent of the half load zone ψ_l and the load distribution ε can be expressed as follows:

$$\psi_l = \cos^{-1}(1 - 2\varepsilon) \quad (18)$$

Furthermore, because the angle between two adjacent rollers is the unit azimuth angle β , the value of k depends on how many β are contained in ψ_l :

$$k = \left\lfloor \frac{\psi_l}{\beta} \right\rfloor = \left\lfloor \frac{\cos^{-1}(1 - 2\varepsilon)}{\beta} \right\rfloor \quad (19)$$

When $\psi_l < \beta$ i.e. $\varepsilon < (1 - \cos \beta) / 2$, there is only one rolling element participating in the load transfer and $k = 0$. Introducing $k = 0$ into Eq. (17), the values of $J_r(\varepsilon)$ when only one rolling element participates in the load transfer can be calculated as follows:

$$J_r(\varepsilon) = \frac{1}{Z} \quad (20)$$

When $\psi_l > \beta$ i.e. $\varepsilon > (1 - \cos \beta) / 2$, according to the initial assumptions in this paper, the load distribution is symmetrical with respect to the line of loading direction. Thus,

$$\cos \varphi_k = \cos \varphi_{Z-k} \quad (21)$$

Then, Eq. (17) can be simplified as

$$J_r(\varepsilon) = \frac{1}{Z} \left\{ 1 + 2 \sum_{j=1}^k \left[1 - \frac{1}{2\varepsilon} (1 - \cos \varphi_j) \right]^n \cos \varphi_j \right\} \quad (22)$$

In summary, $J_r(\varepsilon)$ can be computed from Eq. (23):

$$J_r(\varepsilon) = \frac{1}{Z}, \quad 0 < \varepsilon < (1 - \cos \frac{2\pi}{Z}) / 2 \quad (23a)$$

$$J_r(\varepsilon) = \frac{1}{Z} \left\{ 1 + 2 \sum_{j=1}^k \left[1 - \frac{1}{2\varepsilon} (1 - \cos \varphi_j) \right]^n \cos \varphi_j \right\}, \quad (1 - \cos \frac{2\pi}{Z}) / 2 \leq \varepsilon < 1 \quad (23b)$$

$$J_r(\varepsilon) = \frac{1}{Z} \sum_{j=0}^{j=Z-1} \left[1 - \frac{1}{2\varepsilon} (1 - \cos \varphi_j) \right]^n \cos \varphi_j, \quad \varepsilon \geq 1 \quad (23c)$$

Eq. (23) shows that $J_r(\varepsilon)$ is actually affected by the number of rolling elements. For a given bearing, Z and n are fixed, and a value of ε corresponds to a value of $J_r(\varepsilon)$ for $\varepsilon > 0$. To obtain the curve of $J_r(\varepsilon)$ varying with ε , ε is considered the independent variable with an initial value and increment of both 0.0001 and no more than the constant C . The constant C is defined as the maximum value of ε during the calculation of $J_r(\varepsilon)$. A judgement is needed that if there is only one loaded rolling element. If only one rolling element is loaded, then $J_r(\varepsilon)$ is equal to $1/Z$. With the increase of ε , when there is more than one rolling element taking part in the transfer of F_r , $J_r(\varepsilon)$ can be calculated by Eq. (23b) or (23c). The parameter k in Eq. (23b) is first assumed to be 1. When $(1 - \cos \beta) / 2 \leq \varepsilon < 1$, if ψ_i is less than 2β , there are three rolling elements loaded. If ψ_i is no less than 2β , k is added to 2, and the process mentioned above is repeated. The solving procedure to calculate $J_r(\varepsilon)$ is expressed in a flowchart shown in Figure 6.

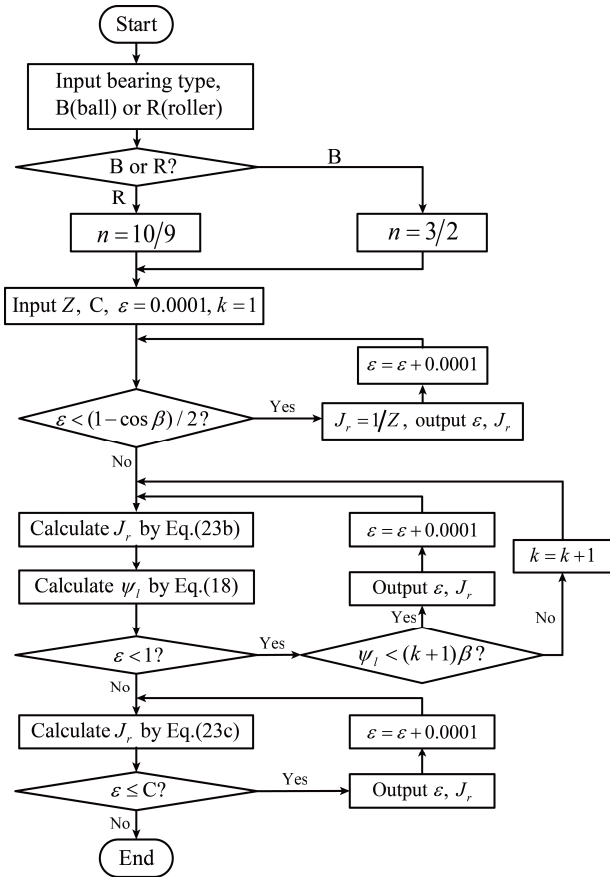


Figure 6 Calculation flowchart of the radial load distribution integral by the discrete method.

4.2 Examples for the Corrected Radial Load Distribution Integral

Figure 7 shows the curves of the corrected radial load distribution integral varying with ε . Eight values of the number of rolling elements Z are considered as examples. The black and red points are the values of Harris integral [1]. It is found that when $\varepsilon < 1$ i.e. the angular extent of the load zone is less than 360 degrees, the corrected radial load distribution integral differs from Harris integral and actually varies with the number of rolling elements, while the corrected integral is almost the same with Harris integral and not affected by the number of rolling elements when $\varepsilon > 1$ i.e. all the rolling elements in a bearing participate in the radial load transfer. Furthermore, as shown in the enlarged view (a) in Figure 7, the corrected curves introduce the values of $J_r(\varepsilon)$ corresponding to $0 < \varepsilon < 0.1$, which cannot be given by Harris integral. It denotes that the corrected radial load distribution integral makes it possible to calculate the load distribution of a bearing with a small load zone (less than 73.74 degrees). Besides, as shown in the enlarged view (b) in Figure 7, it is suggested that the effect of the number of rolling elements on the integral $J_r(\varepsilon)$ is severer for line contact than point contact when $\varepsilon < 1$, which explains why the values and fluctuation of the error for roller bearing are greater than for ball bearing in Figure 2.

In order to illustrate the trend of the corrected radial load distribution integral varying with the scope of the load zone, the corrected curve of line contact and $Z=10$ is chosen as an example and shown in Figure 8a. The black curve is the corrected integral while the red curve is Harris integral for line contact in Figure 8a. It is shown that some obvious turning points exist in the corrected curve corresponding to some specific load distribution factor ε . According to the calculation flow of the corrected $J_r(\varepsilon)$, every time the value of k increases, a turning point appears in the curves of the corrected $J_r(\varepsilon)$. These turning points divide the corrected curve into six load phases, phase I to VI. These phases exactly correspond to the six load phases shown in Figure 4. As shown in Figure 8a, the corrected $J_r(\varepsilon)$ remains the value of 0.1 in phase I where Harris integral curve fails to give the value of $J_r(\varepsilon)$. In phase II to V, the corrected integral curve and Harris integral curve do not coincide at most values of ε except for some intersections, while these two curves almost absolutely coincide in phases VI. Figure 8b shows the difference between the corrected radial load distribution integral and Harris integral which represents the degree of correction to Harris integral. It is found that the variation trend of the difference $\Delta J_r(\varepsilon)$ vs. ε in Figure 8b is absolutely the same with that of the

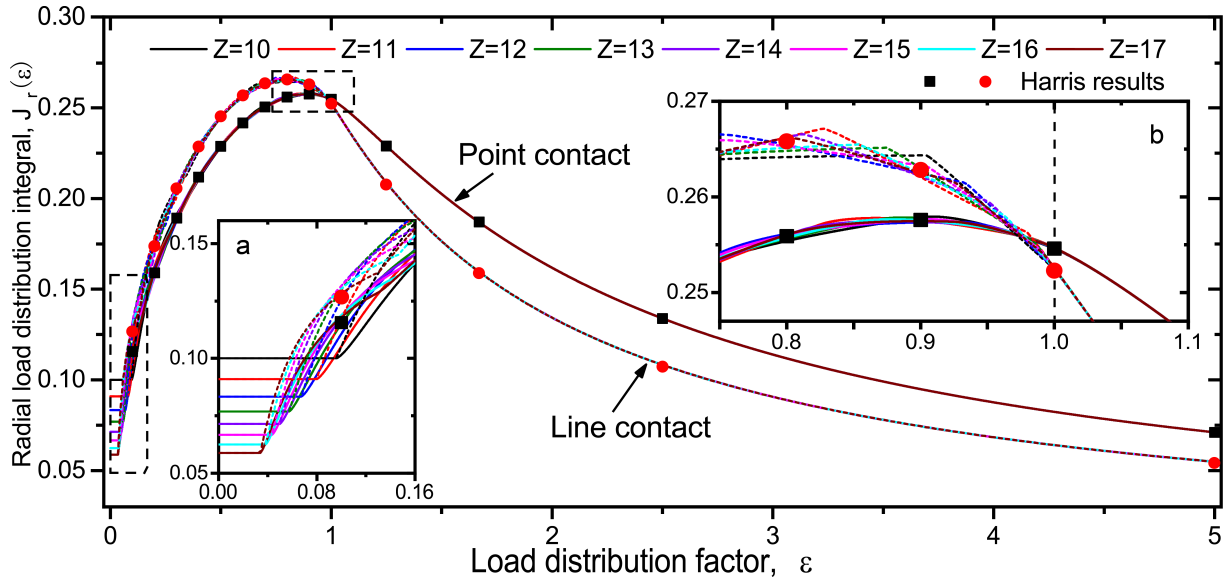


Figure 7 Calculation flowchart of the radial load distribution integral by the discrete method.

error caused by Harris integral vs. ε in Figure 5. Moreover, comparing the values of the difference $\Delta J_r(\varepsilon)$ and the error caused by Harris integral, it is shown that, for a roller bearing with 10 rollers, a deviation of about 0.02 in radial load distribution integral can cause a calculation error of nearly 20%, which suggests the accuracy of the radial load distribution integral is significant for calculating the load distribution accurately.

comparison and (b) difference.

To illustrate the influence of the rolling element number to the radial load distribution integral when $\varepsilon < 1$, the corrected $J_r(\varepsilon)$ curves of $Z = 10 \sim 17$ are shown in Figure 9(a)~(h) respectively. The number of the load phases increase from five for $Z = 10$ to nine for $Z = 17$ in Figure 9. It is demonstrated that the number of the turning points as well as the load phases increase with the increase of Z , and is equal to $\lceil Z/2 \rceil$. This effect of the rolling element number on the divided phases is caused by the variation of the unit azimuth angle β calculated by Eq. (1). As shown in Eq. (1), the unit azimuth angle β decreases with the increase of Z . Then according to Eq. (23a), the scope of phase I of $J_r(\varepsilon)$ becomes narrower with the increase of Z . Furthermore, when $(1 - \cos \beta)/2 \leq \varepsilon < 1$, for a fixed value of ε i.e. a fixed scope of load zone, more rolling elements participate in the load transfer with the decrease of β . It manifests that, with the increase of the number of rolling elements, the same load phase tends to be narrower and move toward smaller values of ε , and new load phases with more active rolling elements appear. Therefore, the number of the load phases increases with the increase of Z . Moreover, although the same load phase tends to be narrower with the increase of Z , for a fixed number of rolling element, different phases correspond to a same angle range of 2β except for the last load phase. As shown in Figure 10, according to the assumption 4, there is a rolling element between two adjacent unit azimuth angles located at the top of a radial bearing with even numbers of rolling element, while there

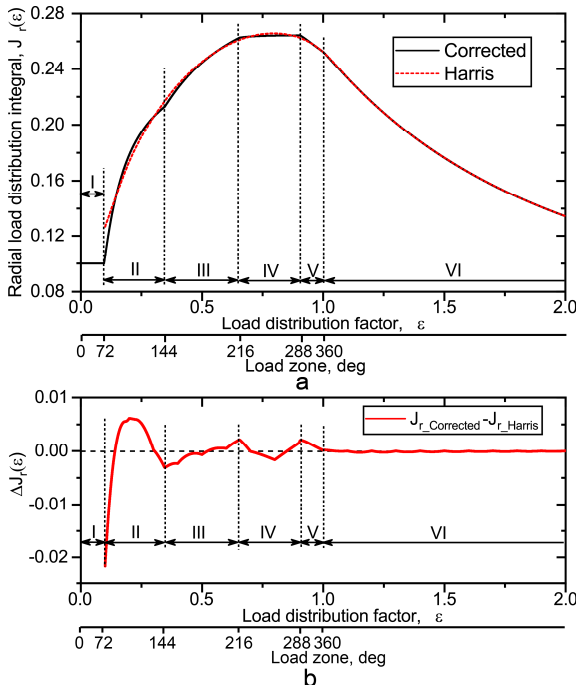


Figure 8 The corrected radial load distribution integral and Harris integral for a radial roller bearing with 10 rollers, (a)

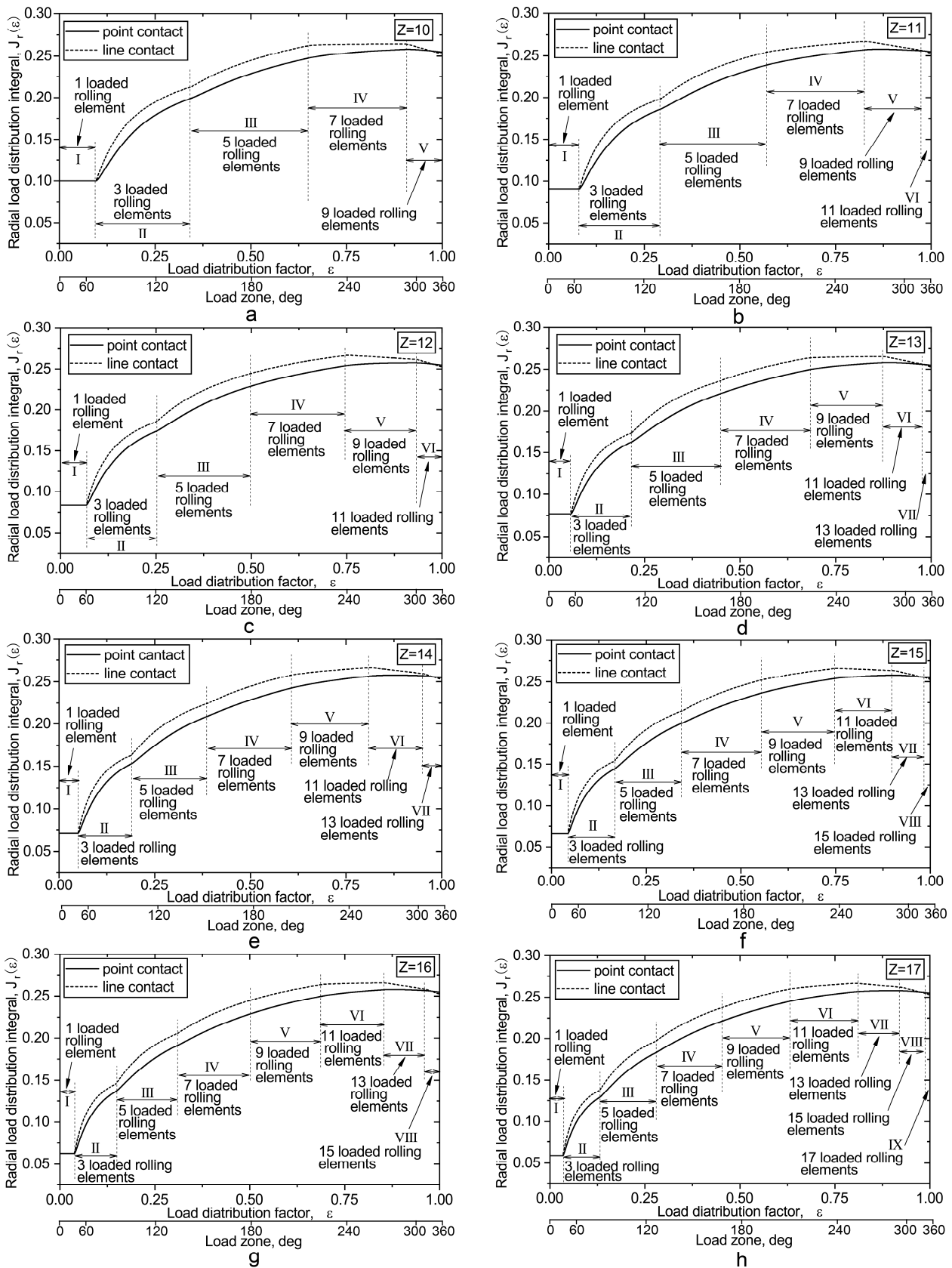


Figure 9 The corrected radial load distribution integral for point and line contact with 10-17 rolling elements corresponding to (a)-(h)

respectively.

is a unit azimuth angle between two adjacent rolling elements located at the top of a radial bearing with odd numbers of rolling element. Therefore, the angle range of the last load phases in Figure 9(a)-(h) is equal to 2β for even numbers of rolling element and equal to β for odd numbers of rolling element.

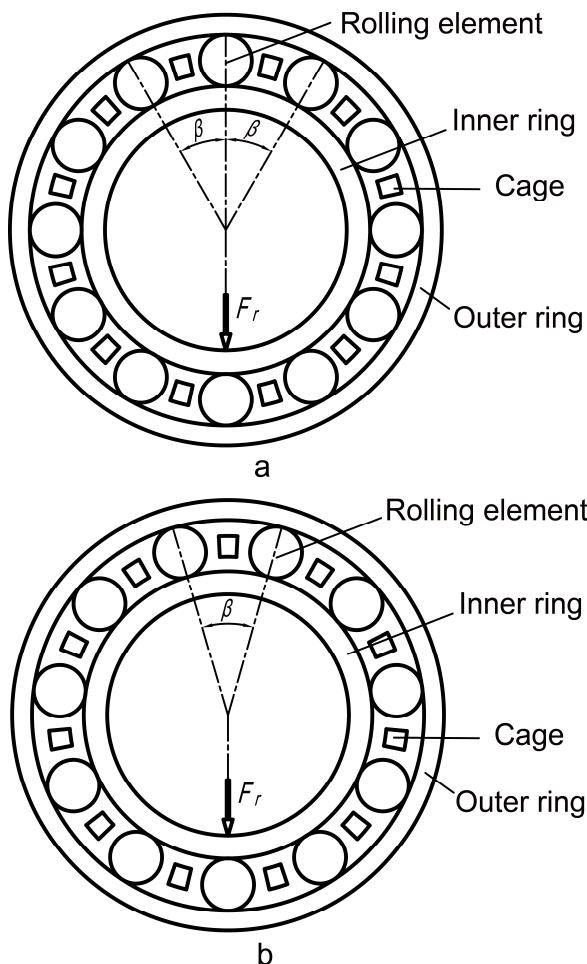


Figure 10 The Schematic view of the radial bearing with (a) even number of rolling elements and (b) odd number of rolling elements.

According to the statements above, there are some characteristics of the corrected integral:

1) The corrected radial load distribution integral makes it possible to calculate the load distribution of a bearing with a small load zone (less than 73.74 degrees) caused by a light external load or a great radial clearance.

2) The corrected radial load distribution integral is affected by the total number of rolling element in a radial bearing.

3) For a bearing with a given number of rolling element, the corrected radial load distribution integral shown in Figure 9 can be used to intuitively ensure the number of rolling element participating in the load transfer and the extent of the load zone.

5 Numerical Examples and Discussion

Some specific numerical examples for the calculation of the radial load distribution are given to illustrate the performance of the proposed correction of the radial load distribution integral. The conditions of the radial load distribution in these examples cover both radial ball and roller bearings with positive and negative clearances under different loads. Moreover, the results of the calculation by the corrected radial load distribution integral are compared with those calculated by Harris integral to show the improvement of the calculation accuracy.

A single row deep groove ball bearing 6209 with odd number of rolling elements and a single row cylindrical roller bearing NU209 with even number of rolling elements are considered in the numerical examples. The parameters of the ball and roller bearings for the numerical calculation are shown in Table 1. The radial clearances shown in Table 1 are the initial clearance chosen from the Rolling Bearing Catalogue of SKF [27]. An interference fitting clearance of -0.010 mm is chosen as the negative clearance for both ball and roller bearings in the numerical examples. Three values of the external radial load F_r are introduced to the calculation. According to these parameters in Table 1, the numerical results of the ball and roller bearings calculated by the corrected $J_r(\varepsilon)$ and Harris $J_r(\varepsilon)$ are displayed in Tables 2-5, respectively. The error of the results here is defined as Eq. (15).

Table 1 Parameters of ball bearings 6209 and roller bearing NU209 [1][27] for the numerical examples

| Ball bearings 6209 | | | | | | | Roller bearings NU209 | | |
|--------------------|-----|----------|------------|------------|------------|------------|-----------------------|-----|----------|
| P_d (mm) | Z | D (mm) | d_i (mm) | d_o (mm) | r_i (mm) | r_o (mm) | P_d (mm) | Z | l (mm) |
| 0.015 | 9 | 12.700 | 52.292 | 77.706 | 6.600 | 6.600 | 0.040 | 14 | 9.601 |

Table 2 Comparison of the numerical results calculated by the corrected radial load distribution integral and Harris integral for the ball bearing with 0.015mm clearance

| | Calculation by corrected integral | | | Calculation by Harris integral | | |
|------------------|-----------------------------------|----------|----------|--------------------------------|----------|----------|
| | 1000 | 5000 | 10000 | 1000 | 5000 | 10000 |
| F_r (N) | 1000 | 5000 | 10000 | 1000 | 5000 | 10000 |
| ε | 0.3178 | 0.4140 | 0.4414 | 0.3188 | 0.4140 | 0.4413 |
| F_0 (N) | 565.102 | 2589.310 | 5073.518 | 582.343 | 2591.211 | 5064.317 |
| F_1 (N) | 283.859 | 1573.419 | 3196.930 | 293.329 | 1574.656 | 3190.693 |
| F_2 (N) | | 0.215 | 82.078 | | 0.230 | 81.477 |
| <i>Error</i> (%) | 0 | 0 | 0 | 3.175 | 0.076 | -0.190 |

Table 3 Comparison of the numerical results calculated by the corrected radial load distribution integral and Harris integral for the ball bearing with -0.010mm clearance

| | Calculation by corrected integral | | | Calculation by Harris integral | | |
|------------------|-----------------------------------|----------|----------|--------------------------------|----------|----------|
| | 1000 | 5000 | 10000 | 1000 | 5000 | 10000 |
| F_r (N) | 1000 | 5000 | 10000 | 1000 | 5000 | 10000 |
| ε | 0.9204 | 0.5876 | 0.5511 | 0.9213 | 0.5878 | 0.5512 |
| F_0 (N) | 432.585 | 2320.970 | 4728.940 | 431.835 | 2311.925 | 4710.094 |
| F_1 (N) | 352.798 | 1663.600 | 3306.271 | 352.258 | 1657.352 | 3293.319 |
| F_2 (N) | 176.981 | 375.306 | 592.111 | 176.877 | 374.3567 | 590.199 |
| F_3 (N) | 34.469 | | | 34.622 | | |
| <i>Error</i> (%) | 0 | 0 | 0 | -0.167 | -0.377 | -0.393 |

Table 4 Comparison of the numerical results calculated by the corrected radial load distribution integral and Harris integral for the roller bearing with 0.040mm clearance

| | Calculation by corrected integral | | | Calculation by Harris integral | | |
|------------------|-----------------------------------|----------|----------|--------------------------------|----------|----------|
| | 1000 | 5000 | 10000 | 1000 | 5000 | 10000 |
| F_r (N) | 1000 | 5000 | 10000 | 1000 | 5000 | 10000 |
| ε | 0.0832 | 0.1932 | 0.2533 | — | 0.1904 | 0.2551 |
| F_0 (N) | 602.323 | 2157.290 | 3716.601 | — | 2104.554 | 3786.782 |
| F_1 (N) | 220.639 | 1552.340 | 2918.810 | — | 1505.991 | 2979.454 |
| F_2 (N) | | 36.408 | 821.021 | — | 14.402 | 855.069 |
| <i>Error</i> (%) | 0 | 0 | 0 | — | -3.276 | -2.118 |

Table 5 Comparison of the numerical results calculated by the corrected radial load distribution integral and Harris integral for the roller bearing with -0.010mm clearance

| | Calculation by corrected integral | | | Calculation by Harris integral | | |
|------------------|-----------------------------------|----------|----------|--------------------------------|----------|----------|
| | 1000 | 5000 | 10000 | 1000 | 5000 | 10000 |
| F_r (N) | 1000 | 5000 | 10000 | 1000 | 5000 | 10000 |
| ε | 3.506 | 1.095 | 0.739 | 3.506 | 1.095 | 0.741 |
| F_0 (N) | 917.431 | 1522.860 | 2703.460 | 916.927 | 1522.977 | 2694.401 |
| F_1 (N) | 903.046 | 1446.533 | 2503.171 | 902.549 | 1446.670 | 2495.107 |
| F_2 (N) | 862.863 | 1234.861 | 1950.810 | 862.387 | 1235.000 | 1945.472 |
| F_3 (N) | 805.128 | 935.456 | 1180.900 | 804.683 | 935.597 | 1179.300 |
| F_4 (N) | 741.531 | 614.291 | 386.704 | 741.118 | 614.432 | 388.717 |
| F_5 (N) | 684.694 | 388.872 | | 684.311 | 339.011 | |
| F_6 (N) | 645.633 | 160.368 | | 645.271 | 160.501 | |
| F_7 (N) | 631.749 | 100.575 | | 631.394 | 100.703 | |
| <i>Error</i> (%) | 0 | 0 | 0 | -0.052 | 0.002 | -0.318 |

It is shown that the errors of the results calculated by the corrected $J_r(\varepsilon)$ are all nil, while the errors of the results calculated by Harris $J_r(\varepsilon)$ are obvious and vary with ε following the rules illustrated in Section 3. It is indicated that the corrected $J_r(\varepsilon)$ can be used to obtain a more accurate radial load distribution than the value of $J_r(\varepsilon)$ given by Harris shown in *Figure 7.2* in Ref. [1]. Moreover, as shown in Table 4, when $P_d = 0.040\text{mm}$ and $F_r = 1000\text{N}$, the calculation by the corrected radial load distribution integral shows an accurate solution, while the calculation by Harris integral failed to obtain the load distribution due to the defect of the values of Harris $J_r(\varepsilon)$ when $0 < \varepsilon < 0.1$.

Under the situation of a small load zone caused by a light external load or a great radial clearance, the load distribution plays a significant role in the studies of skidding behaviour [26,28] and the fatigue life [14] of bearings. The sliding velocities of the rollers are considered to exist under light external loads and vary with the radial load distribution in the bearing by Tu et al. [26] and Han et al. [28]. Moreover, the skidding of the roller at the entry of the loaded zone is likely to cause wear on the raceway surface [26]. Thus, accurate calculation of the load distribution under light load condition can be used to ensure the skidding states of the rollers and the locations of the possible wear. Furthermore, a greater radial clearance will cause a kind of load distribution with a smaller load zone and a greater maximum rolling element load. Then, the fatigue life of the bearing will decrease under this kind of load distribution [14]. Therefore, accurate calculation of the load distribution under great clearance condition contributes to avoiding early failure caused by improper assembly. Besides, according to the calculation method of fatigue life proposed by Lundberg and Palmgren [25], the basic dynamic capacity of a bearing is calculated by the radial load distribution and the radial load distribution integral. It reveals that the errors of radial load distribution and radial load distribution integral will be transferred and accumulated in the calculation of the fatigue life of bearings. Thus, the correction of the radial load distribution integral and its contribution on the accurate calculation of the load distribution are significant for predicting the fatigue life accurately especially for the light load or great clearance conditions.

6 Conclusions

Based on the analysis of the error from Harris method to calculate the radial load distribution in radial bearings, the

radial load distribution integral for radial bearings was corrected in this paper. The calculation of the corrected $J_r(\varepsilon)$ was divided into three stages according to the values of the load distribution factor ε . Some numerical examples were used to illustrate the characteristics and application of the corrected radial load distribution integral. The following conclusions were obtained:

- (1) The errors of Harris method are affected by the load distribution factor ε and absolutely caused by the inaccurate values of the radial load distribution integral evaluated numerically by Harris.
- (2) The corrected radial load distribution integral is effective for calculating the load distribution under the situation of a small load zone caused by a light external load or a great radial clearance ($0 < \varepsilon < 0.1$), which cannot be solved by Harris integral. Under this small load zone situation, the corrected radial load distribution integral contributes to ensuring the bearing skidding states and avoiding early failure caused by improper assembly.
- (3) The corrected radial load distribution integral shows the effect of the rolling element number on the values of $J_r(\varepsilon)$ when the load distribution factor ε is less than 1 i.e. not all rolling elements participate in the load transfer.
- (4) For a given number of rolling elements, the corrected curves of $J_r(\varepsilon)$ versus ε can be divided into some load phases according to the number of rolling elements and used to intuitively ensure the radial load distribution in the bearing.
- (5) The accuracy of the integral method to calculate the radial load distribution is improved by the corrected radial load distribution integral, which are significant for predicting the fatigue life more accurately according to the theory of Lundberg-Palmgren.

7 Declaration

Acknowledgements

Not applicable

Funding

Supported by the Joint Funds of the National Natural Science Foundation of China [Grant No. U1834202].

Availability of data and materials

The datasets supporting the conclusions of this article are included within the article.

Authors' contributions

Yu Hou analysed the error of Harris integral, and was a major contributor in writing the manuscript. Yi Yin wrote the computer program for correcting the integral of radial load distribution. All authors read and approved the final manuscript.

Competing interests

The authors declare no competing financial interests.

Consent for publication

Not applicable

Ethics approval and consent to participate

Not applicable

References

- [1] T A Harris, M N Kotzalas. *Rolling Bearing Analysis: Essential Concepts of Bearing Technology*, 5th Edition, CRC Press, Boca Raton, FL, 2007.
- [2] R Tomovic. Investigation of the Effect of Rolling Bearing Construction on Internal Load Distribution and the Number of Active Rolling Elements. *Advanced Materials Research*, 2013, 633: 103–116.
- [3] S Glodež, R Potočnik, J Flašker. Computational Model for Calculation of Static Capacity and Lifetime of Large Slewing Bearing's Raceway. *Mechanism and Machine Theory*, 2012, 47: 16–30.
- [4] R Potočnik, P Göncz, S Glodež. Static Capacity of a Large Double Row Slewing Ball Bearing with Predefined Irregular Geometry. *Mechanism and Machine Theory*, 2013, 64: 67–79.
- [5] D Petersen, C Howard, Z Prime. Varying Stiffness and Load Distributions in Defective Ball Bearings: Analytical Formulation and Application to Defect Size Estimation. *Journal of Sound and Vibration*, 2015, 337: 284–300.
- [6] D Brie. Modelling of the Spalled Rolling Element Bearing Vibration Signal: An Overview and Some New Results. *Mechanical Systems and Signal Processing*, 2000, 14(3): 353–369.
- [7] X Zhang, Q Han, Z Peng, F Chu. A Comprehensive Dynamic Model to Investigate the Stability Problems of the Rotor-Bearing System Due to Multiple Excitations. *Mechanical Systems and Signal Processing*, 2016, 70–71: 1171–1192.
- [8] H Xi, H Y Wang, W Han, Y Le, H Xu, W Chen, S N Xu, F C Wang. Contact Trajectory of Angular Contact Ball Bearings under Dynamic Operating Condition. *Tribology International*, 2016, 104: 247–262.
- [9] X Hernot, M Sartor, J Guillot. Calculation of the Stiffness Matrix of Angular Contact Ball Bearings by Using the Analytical Approach. *Journal of Mechanical Design*, 2000, 122(1): 83–90.
- [10] J Liu, C Tang, H Wu, Z Xu, L Wang. An Analytical Calculation Method of the Load Distribution and Stiffness of an Angular Contact Ball Bearing. *Mechanism and Machine Theory*, 2019, 142, 103597.
- [11] D Petersen, C Howard, N Sawalhi, A Moazen Ahmadi, S Singh. Analysis of Bearing Stiffness Variations, Contact Forces and Vibrations in Radially Loaded Double Row Rolling Element Bearings with Raceway Defects. *Mechanical Systems and Signal Processing*, 2015, 50–51: 139–160.
- [12] P Szumiński. Determination of the Stiffness of Rolling Kinematic Pairs of Manipulators. *Mechanism and Machine Theory*, 2007, 42: 1082–1102.
- [13] T A Harris, M N Kotzalas. *Rolling Bearing Analysis: Advanced Concepts of Bearing Technology*, 5th Edition, CRC Press, Boca Raton, FL, 2007.
- [14] F B Oswald, E V Zaretsky, J V Poplawski. Effect of Internal Clearance on Load Distribution and Life of Radially Loaded Ball and Roller Bearings. *Tribology Transactions*, 2012, 55(2): 245–265.
- [15] T Nagatomo, K Takahashi, Y Okamura, T Kigawa, S Noguchi. Effects of Load Distribution on Life of Radial Roller Bearings. *Journal of Tribology*, 2012, 134(2): 021101.
- [16] R Stribeck. Ball Bearings for Various Loads. *ASME Transactions*. 1907, 29: 420–463.
- [17] H Sjövall. The Load Distribution within Ball and Roller Bearings under Given External Radial and Axial Load. *Teknisk Tidskrift Mekanik*, 1933, 9: 97–102. (in Swedish)
- [18] L Houptert. A Uniform Analytical Approach for Ball and Roller Bearings Calculations. *Journal of Tribology*, 1997, 119(4): 851–858.
- [19] R Tomović. Calculation of the Necessary Level of External Radial Load for Inner Ring Support on Q Rolling Elements in a Radial Bearing with Internal Radial Clearance. *International Journal of Mechanical Science*, 2012, 60(1): 23–33.
- [20] X Ren, J Zhai, G Ren. Calculation of Radial Load Distribution on Ball and Roller Bearings with Positive, Negative and Zero Clearance. *International Journal of Mechanical Science*, 2017, 131–132: 1–7.
- [21] N Sawalhi, R B Randall. Simulating Gear and Bearing Interactions in the Presence of Faults. Part II: Simulation of the Vibrations Produced by Extended Bearing Faults. *Mechanical Systems and Signal Processing*, 2008, 22(8): 1952–1966.
- [22] N Sawalhi, R B Randall. Simulating Gear and Bearing Interactions in the Presence of Faults. Part I. The combined Gear Bearing Dynamic Model and the Simulation of Localised Bearing Faults. *Mechanical Systems and Signal Processing*, 2008, 22(8): 1924–1951.
- [23] S Singh, U G Köpke, C Q Howard, D Petersen. Analyses of Contact Forces and Vibration Response for a Defective Rolling Element Bearing Using an Explicit Dynamics Finite Element Model. *Journal of Sound and Vibration*, 2014, 333(21): 5356–5377.
- [24] A Palmgren. *Ball and Roller Bearing Engineering*. 3rd Edition, SKF Industries, Philadelphia, 1959.
- [25] G Lundberg, A Palmgren. Dynamic Capacity of Rolling Bearings. *Acta Polytechnica*, 1947, 1: 3.
- [26] W Tu, Y Luo, W Yu. Investigation of the Dynamic Local Skidding Behaviour of Rollers in Cylindrical Roller Bearings. *Proceedings of the Institution of Mechanical Engineers, Part K: Journal of Multibody Dynamics*, 2019, 233(4): 899–909.
- [27] SKF. *Rolling Bearings Catalogue*. SKF Group, 17000 EN, 2018.
- [28] Q Han, X Li, F Chu. Skidding Behavior of Cylindrical Roller Bearings under Time-Variation Load Conditions. *International Journal of Mechanical Science*, 2018, 135: 203–214.
- [29] D E Brewe, B J Hamrock. Simplified Solution for Elliptical-Contact Deformation between Two Elastic Solids. *Journal of Tribology*, 1977, 99(4): 485–487.

Biographical notes

Yu Hou, born in 1994, is currently a PhD candidate at *School of Mechanical, Electronic and Control Engineering, Beijing Jiaotong University, China*. His research interests include structural health

monitoring and mechanical properties of rolling bearings.
E-mail: 17116391bjtu.edu.cn

Yi Yin, born in 1990, is currently a postdoctoral fellow at *School of Mechanical, Electronic and Control Engineering, Beijing Jiaotong University, China*.

Xi Wang, born in 1976, is currently a professor and a PhD candidate supervisor at *School of Mechanical, Electronic and Control Engineering, Beijing Jiaotong University, China*. His main research interests include structure reliability and optimization of high-speed train.

Tel.: +86 10 51683195; E-mail: wangxi@bjtu.edu.cn

Appendix. Calculation of the Stiffnesses of the Inner and Outer Raceway Contact Deformation

A series of stiffnesses of the inner and outer raceway contact deformation K is calculated as follows [1]:

$$K = \left[\frac{1}{(1/K_i)^{1/n} + (1/K_o)^{1/n}} \right]^n \quad (\text{A.1})$$

where K_i and K_o are the stiffness of the inner and outer raceway contact deformation, respectively. For ball bearings,

$$K_i = 2.15 \times 10^5 \left(\sum \rho_i \right)^{-1/2} \left(\delta_i^* \right)^{-3/2} \quad (\text{A.2})$$

$$K_o = 2.15 \times 10^5 \left(\sum \rho_o \right)^{-1/2} \left(\delta_o^* \right)^{-3/2} \quad (\text{A.3})$$

where $\sum \rho_i$ and $\sum \rho_o$ are the summations of the inner and outer raceway curvatures, respectively. For the ball bearing shown in Figure 1, according to Hertz elastic contact theory:

$$\sum \rho_i = \frac{2}{d_i} - \frac{1}{r_i} + \frac{2}{D} + \frac{2}{D} \quad (\text{A.4})$$

$$\sum \rho_o = -\frac{2}{d_o} - \frac{1}{r_o} + \frac{2}{D} + \frac{2}{D} \quad (\text{A.5})$$

where d_i , d_o and r_i , r_o are raceway diameters and raceway groove curvature radii, respectively. The parameters δ_i^* and δ_o^* are the raceway dimensionless contact parameters, which are determined by the geometry

of the ball and raceway contact. The calculation of δ^* is illustrated in detail in the Appendix.

For the point contact of two elastic solids, δ^* is one of the contact dimensionless quantities. It is expressed as [1]:

$$\delta^* = \frac{2F}{\pi} \left(\frac{\pi}{2\kappa^2 E} \right)^{1/3} \quad (\text{A.6})$$

where κ is the ratio of the length to the short half axis of the contact ellipse. F and E are the complete elliptic integrals of the first and second kinds, respectively,

$$F = \int_0^{\pi/2} \left[1 - \left(1 - \frac{1}{\kappa^2} \right) \sin^2 \phi \right]^{-1/2} d\phi \quad (\text{A.7})$$

$$E = \int_0^{\pi/2} \left[1 - \left(1 - \frac{1}{\kappa^2} \right) \sin^2 \phi \right]^{1/2} d\phi \quad (\text{A.8})$$

Simplified approximations for κ , F and E were obtained by Brewe and Hamrock [29] using a least squares method of linear regression. The formulas are as follows:

$$\kappa \approx 1.0339 \left(\frac{R_y}{R_x} \right)^{0.636} \quad (\text{A.9})$$

$$E \approx 1.0003 + \frac{0.5968}{\left(\frac{R_y}{R_x} \right)} \quad (\text{A.10})$$

$$F \approx 1.5277 + 0.6023 \ln \left(\frac{R_y}{R_x} \right) \quad (\text{A.11})$$

The errors of these equations were analysed. For $1 \leq \kappa \leq 10$, the errors in the calculation of κ are less than 3%. The errors on E are essentially nil except at $\kappa = 1$ and in the vicinity where they are less than 2%. The errors on F are essentially nil except at $\kappa = 1$ and in the vicinity where they are less than 2.6%. R_x and R_y are the directional equivalent radii of the major axis direction and minor axis direction of the contact, respectively. For the given ball bearing shown in Figure 1,

$$\frac{R_{yi}}{R_{xi}} = \frac{\frac{2}{d_i} + \frac{2}{D}}{-\frac{1}{r_i} + \frac{2}{D}} \quad (\text{A.12})$$

Therefore, the inner and outer raceway dimensionless contact parameters δ_i^* and δ_o^* can be calculated by Eq. (A.6).

For roller bearings,

$$\frac{R_{yo}}{R_{xo}} = \frac{-\frac{2}{d_o} + \frac{2}{D}}{-\frac{1}{r_o} + \frac{2}{D}} \quad (\text{A.13})$$

$$K_i = K_o = 8.06 \times 10^4 l^{8/9} \quad (\text{A.14})$$

Figures

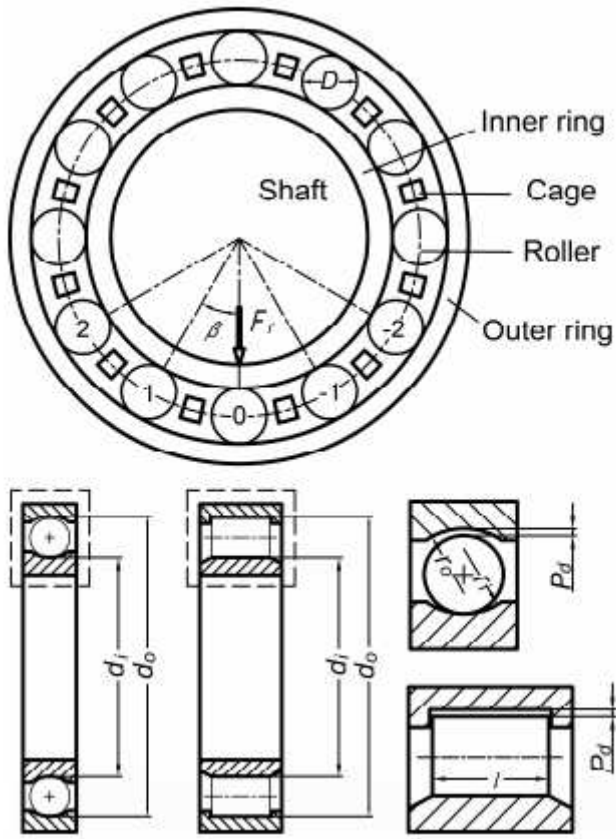


Figure 1

The structure and geometric parameters of the radial ball and roller bearing.

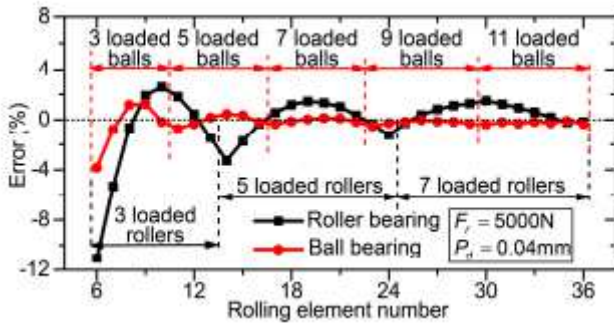


Figure 2

Errors of Harris method vs. the total number of rolling elements.

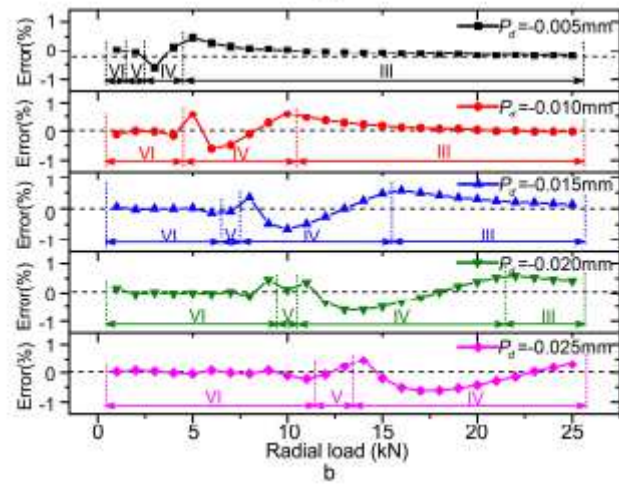
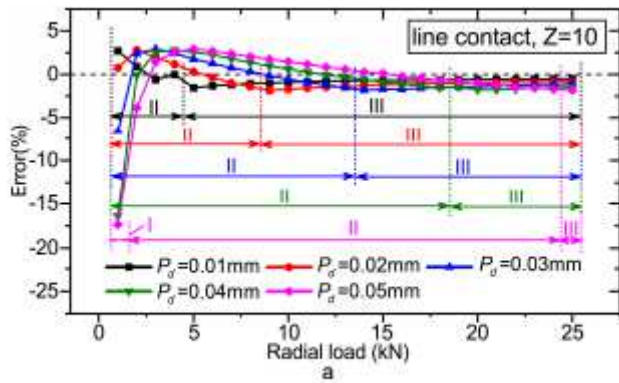


Figure 3

Errors of Harris method vs. the external radial loads and radial clearances, (a) positive clearances and (b) negative clearances.

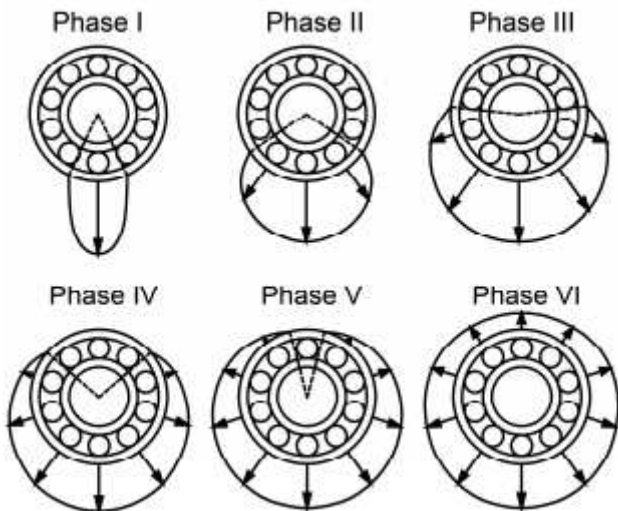


Figure 4

Six load phases of the radial bearing with 10 rolling elements.

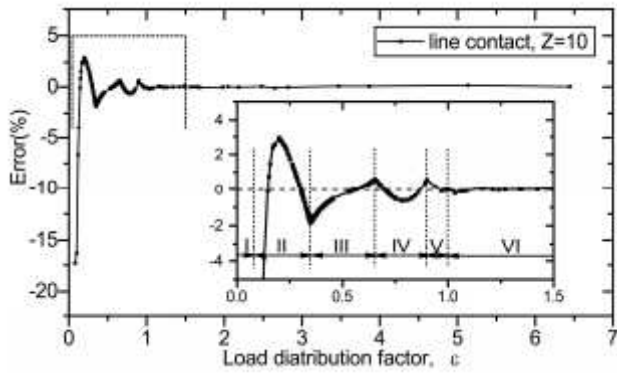


Figure 5

Error of Harris method vs. the load distribution factor for a roller bearing with 10 rollers.

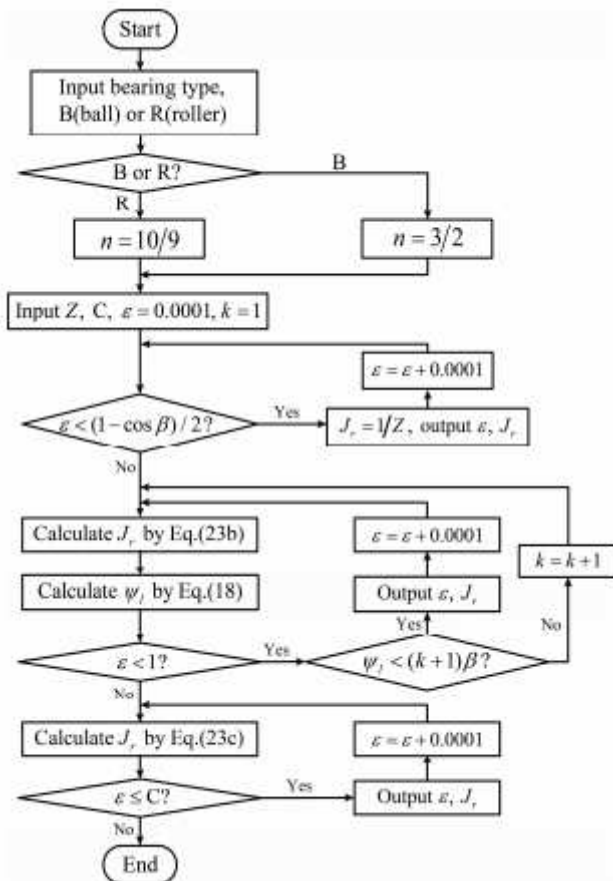


Figure 6

Calculation flowchart of the radial load distribution integral by the discrete method.

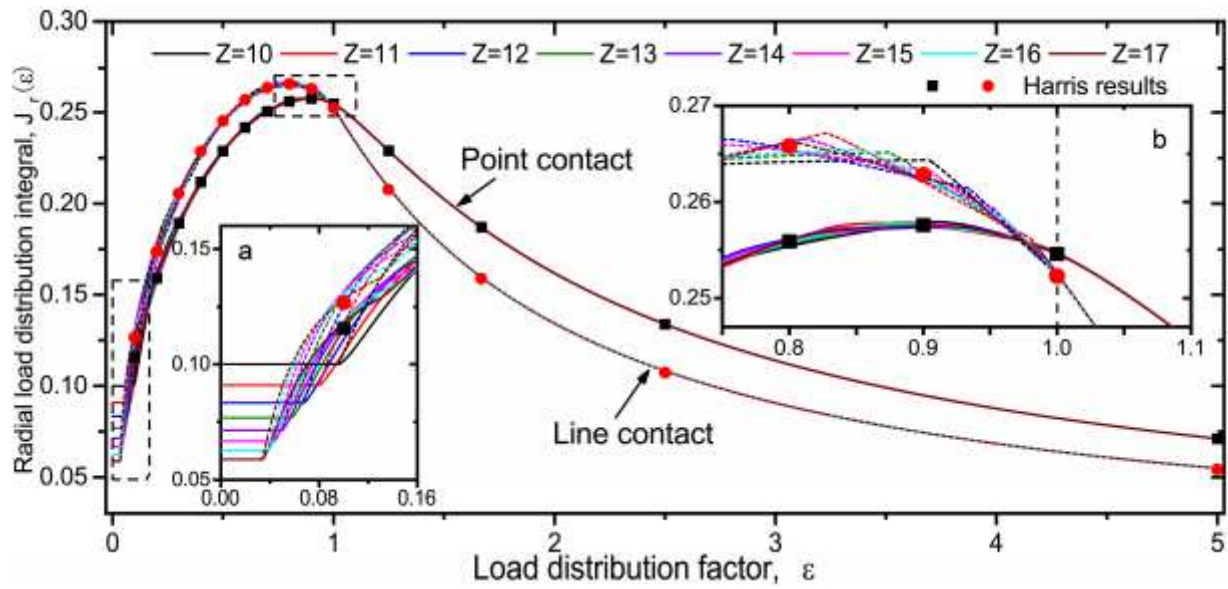


Figure 7

Calculation flowchart of the radial load distribution integral by the discrete method.

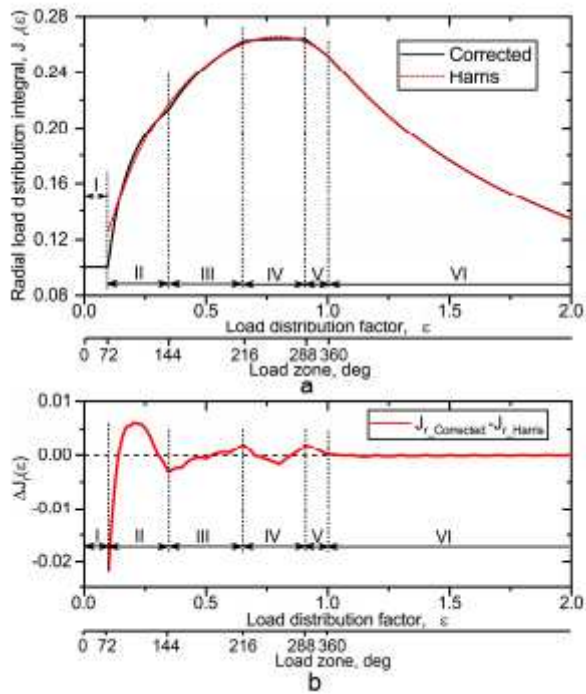


Figure 8

The corrected radial load distribution integral and Harris integral for a radial roller bearing with 10 rollers, (a) comparison and (b) difference.

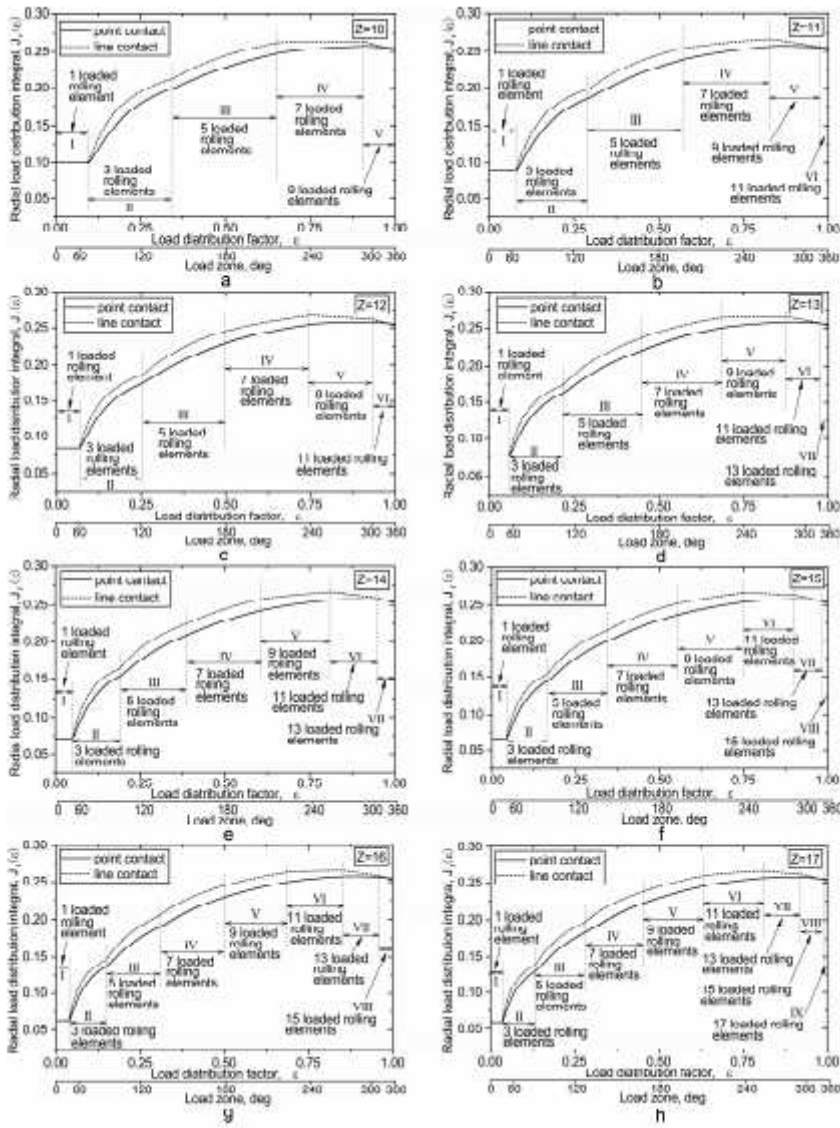


Figure 9

The corrected radial load distribution integral for point and line contact with 10-17 rolling elements corresponding to (a)-(h) respectively.

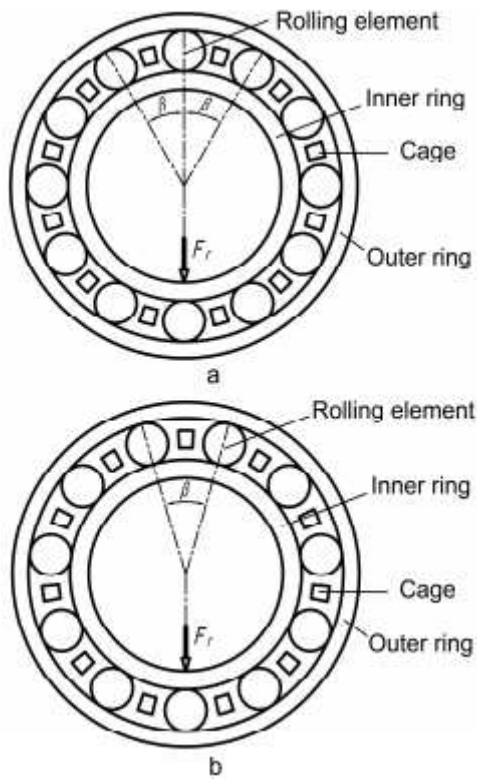


Figure 10

The Schematic view of the radial bearing with (a) even number of rolling elements and (b) odd number of rolling elements.